


Myositis with sarcoplasmic inclusions in Nakajo–Nishimura syndrome: a genetic inflammatory myopathy

T. Ayaki* , K. Murata†, N. Kanazawa‡, A. Uruha§¶**, K. Ohmura††, K. Sugie‡‡, S. Kasagi§§, F. Li¶¶, M. Mori***, R. Nakajima†††, T. Sasai†††, I. Nishino§, S. Ueno‡‡‡, M. Urushitani††††, F. Furukawa‡, H. Ito*** and R. Takahashi*

*Department of Neurology, Kyoto University Graduate School of Medicine, Kyoto, †Center for Educational Research and Development, Wakayama Medical University, ‡Department of Dermatology, Wakayama Medical University, Wakayama, §Department of Neuromuscular Research, National Institute of Neuroscience, National Center of Neurology and Psychiatry (NCNP), ¶Department of Genome Medicine Development, Medical Genome Center, Kodaira, Tokyo, **Department of Neuropathology, Charité - Universitätsmedizin, Berlin, Germany, ††Department of Rheumatology and Clinical Immunology, Graduate School of Medicine, Kyoto University, Sakyo-ku, Kyoto, ‡‡Department of Neurology, Nara Medical University School of Medicine, Kashihara, Nara, §§Minato Motomachi Internal Medicine Clinic, Kobe, Hyogo, Japan, ¶¶Department of Neurology, Research Center of Neurology in Second Affiliated Hospital, Key Laboratory of Medical Neurobiology of Zhejiang Province, Zhejiang University School of Medicine, Hangzhou, China, ***Department of Neurology, Wakayama Medical University, Wakayama and ††††Department of Neurology, Shiga University of Medical Science, Seta Tsukinowa-cho, Otsu City, Shiga, Japan

T. Ayaki, K. Murata, N. Kanazawa, A. Uruha, K. Ohmura, K. Sugie, S. Kasagi, F. Li, M. Mori, R. Nakajima, T. Sasai, I. Nishino, S. Ueno, M. Urushitani, F. Furukawa, H. Ito and R. Takahashi (2020) *Neuropathology and Applied Neurobiology* 46, 579–587

Myositis with sarcoplasmic inclusions in Nakajo–Nishimura syndrome: a genetic inflammatory myopathy

Aims: Nakajo–Nishimura syndrome (NNS) is an autosomal recessive disease caused by biallelic mutations in the *PSMB8* gene that encodes the immunoproteasome subunit $\beta 5i$. There have been only a limited number of reports on the clinicopathological features of the disease in genetically confirmed cases. **Methods:** We studied clinical and pathological features of three NNS patients who all carry the homozygous p.G201V mutations in *PSMB8*. Patients' muscle specimens were analysed with histology and immunohistochemistry. **Results:** All patients had episodes of typical periodic fever and skin rash, and later developed progressive muscle weakness

and atrophy, similar to previous reports. Oral corticosteroid was used for treatment but showed no obvious efficacy. On muscle pathology, lymphocytes were present in the endomysium surrounding non-necrotic fibres, as well as in the perimysium perivascular area. Nearly all fibres strongly expressed MHC-I in the sarcolemma. In the eldest patient, there were abnormal protein aggregates in the sarcoplasm, immunoreactive to p62, TDP-43 and ubiquitin antibodies. **Conclusions:** These results suggest that inflammation, inclusion pathology and aggregation of abnormal proteins underlie the progressive clinical course of the NNS pathomechanism.

Keywords: genetic inflammatory myopathy, immunoproteasome subunit $\beta 5i$, myositis, Nakajo–Nishimura syndrome, proteasome subunit beta type 8 gene, proteasome-associated autoinflammatory syndrome

Correspondence: Takashi Ayaki, Department of Neurology, Kyoto University Graduate School of Medicine, 53, Kawahara-Cho, Shogoin, Sakyo-Ku, Kyoto 606-8507, Japan. Tel: +81 75 751 3766; Fax: +81 75 751 4257; E-mail: ayaki520@kuhp.kyoto-u.ac.jp

[Correction added on 23 April 2020, after first online publication: The author names U. Satoshi, U. Makoto, F. Fukumi were listed in the wrong order, and have been corrected in this version to list their given name followed by family name.]

Introduction

Nakajo–Nishimura syndrome (NNS) is an autosomal recessive disorder caused by a homozygous mutation in the proteasome subunit beta type 8 gene (*PSMB8*), which encodes the immunoproteasome subunit $\beta 5i$ [1–3]. Mutant $\beta 5i$ subunit impairs immunoproteasome function, including truncation of abnormal or useless proteins especially during inflammation, leading to the accumulation of ubiquitinated proteins and increase in interferon gamma-induced protein 10 (IP-10) and interleukin-6 (IL-6) by activation of the mitogen-activated protein kinase (MAPK) cascade and JAK-STAT signalling pathway [1,4,5]. The clinical course of NNS is characterized by systemic inflammatory and muscle wasting symptoms in a variety of organs including the skin, joints and skeletal muscle. Patients typically present with a pernio-like rash and periodic high fever in early infancy. In adolescence, they often develop myositis and nodular erythema-like eruptions. This is followed by gradual lipomuscular atrophy and joint contractures, leading to the development of thin appearance in the face, chest and arms as well as elongated clubbed fingers and toes. NNS has been described in Japan, and the approximate number of patients so far is 30. Recently, *PSMB8* has been found to be the causative gene, not only of NNS, but also of chronic atypical neutrophilic dermatosis with lipodystrophy and elevated temperature (CANDLE) syndrome [6], and joint contractures, muscular atrophy, microcytic anaemia and panniculitis-associated lipodystrophy (JMP) syndrome [7,8]. These syndromes are now collectively called proteasome-associated autoinflammatory syndrome (PRAAS). As patients with CANDLE and JMP syndromes have been reported in European and American countries, PRAAS patients seem to be distributed worldwide and may not be extremely rare.

Immunosuppressive therapy with corticosteroids partially alleviates inflammatory symptoms but usually does not prevent lipomuscular atrophy and joint contractures. Patients with NNS usually die in their 40–50s [1]. Although JAK1/2 inhibition with Baricitinib has been recently reported to improve clinical manifestations and inflammatory and IFN biomarkers in patients with CANDLE and those with other interferonopathies [9], available treatments are still limited in PRAAS.

Skin biopsy shows perivascular and peri-adnexal inflammatory changes [1,2]. Skin histology shows the accumulation of ubiquitinated proteins in macrophages

[1]. Another histological finding is an intracellular accumulation of ubiquitinated proteins. Muscle pathology includes inflammatory cell infiltration in the endomysium surrounding vessels and myofibres [10,11]. Myopathic changes in an autopsied sample include rimmed vacuoles, myeloid bodies, cytoplasmic bodies and vascular medial hyperplasia without inflammatory changes [12]. These pathological features characterized by accumulation of abnormal proteins could underlie the progressive clinical course and the refractory response to immunosuppressive therapy in NNS patients. Further pathological analysis has not been reported, possibly due to the limited number of biopsy samples. However, it is necessary to delineate the pathological features to understand the pathomechanism of the progressive clinical course and establish a reasonable therapeutic strategy. A comparison of several cases could elucidate the process of inflammation and muscle fibre degeneration in NNS. We examined muscle pathology of three unrelated NNS patients with the same homozygous p.G201V mutation in *PSMB8*.

Patients

The following three patients were included in this study. All were genetically diagnosed as having NNS based on the presence of a homozygous p.G201V mutation in *PSMB8*, described in a previous report [1].

Case 1

The patient's parents were consanguineous, but there was no family history of collagen vascular diseases. When 10 months old, the patient had a periodic fever and nasal oedematous erythema. At 12 years of age, she developed frostbitten hands and finger deformities. At the age of 19, she experienced joint pains; she was treated with a corticosteroid, which did not show any evident effect. At the age of 24, she developed fatigue and joint pains with periodic fever. She had mild atrophy of the subcutaneous adipose tissue, especially in her face, fingers and upper limbs. Neurologically, no obvious muscle weakness was observed. The patient did not have cognitive impairment. Laboratory tests showed elevated levels of C-reactive protein (CRP: 5.3 mg/dl) and creatine kinase (CK: 361 IU/l). An antinuclear antibody test was positive at a serum dilution of 1:640 (homogenous type). Anti-double strand DNA and anti-SS-B antibody tests

were also positive. A brain computed tomography (CT) scan showed calcification of basal ganglia, and an abdominal CT scan showed hepatosplenomegaly. Skeletal muscle magnetic resonance imaging (MRI) showed patchy T2 high-intensity lesion in the thigh muscle and a thigh muscle biopsy was performed. The muscle specimen was fixed in 10% buffered formalin and paraffin-embedded blocks were prepared [11].

Case 2

The patient's parents were consanguineous, but there was no family history of collagen vascular diseases. At the age of 2 months, he developed frostbitten erythema on his face and limbs. At the age of 6 years, he developed mild weakness in the limbs, especially in his left arm. This patient had no history of cognitive impairment or hepatosplenomegaly. At the age of 18, he showed elevated levels of serum CK (600–700 IU/l) and erythrocyte sedimentation rate (ESR: 25/54 mm/h). An antinuclear antibody test was negative, as well as autoantibodies including anti-Jo-1, -RNP and -double strand DNA. A brain CT scan revealed calcification of the basal ganglia. A left rectus femoris muscle biopsy was performed and a frozen specimen was prepared. The patient was treated with a corticosteroid, which did not show any evident effect. At the age of 31, he developed mild muscle

weakness of the upper limbs (the Medical Research Council [MRC] manual muscle testing showed MRC Grade 4; other muscles showed MRC Grade 5) and erythema on his face and limbs. Electromyography showed myogenic changes in the upper and lower limbs.

Case 3

At 2 years of age, the patient developed facial frostbitten erythema. He was treated with a corticosteroid; the eruption disappeared once but appeared again later. Muscle weakness of upper and lower limbs continued to progress until the age of 29. The patient also developed atrophy in his face and upper limbs as well as muscle weakness in the upper limbs (MRC Grade 4). This patient had a history of hepatosplenomegaly and cognitive impairment. Laboratory tests showed normal levels of CK, CRP and ESR. An antinuclear antibody test was positive at a 1:40 serum dilution. An anti-double strand DNA antibody test was also positive. A brain CT scan showed basal ganglia calcification. Electromyography showed myogenic changes in the upper limbs. Muscle MRI showed T2 high-intensity lesion in the upper limbs. A right triceps brachii muscle biopsy was performed. Both frozen and formalin specimens were prepared.

The clinical data of the three patients are summarized in Table 1.

Table 1. Cohort characteristics

	Case 1	Case 2	Case 3
<i>PSMB8</i> mutation site	G201V homozygous mutation	G201V homozygous mutation	G201V homozygous mutation
Onset age	10 months	2 months	2 y.o
Systemic symptoms	Periodic fever, skin rash, joint deformity, muscle weakness	Periodic fever, skin rash, joint deformity, muscle weakness	Periodic fever, skin rash, joint deformity, muscle weakness
Corticosteroid therapy before biopsy	+	+	+
Blood laboratory data at age of muscle biopsy	CK 361 IU/l, CRP 5.3 mg/dl	CK 600-700 IU/l, ESR 25 mm/h	CK, CRP, ESR within normal limit
Age of biopsy, site of biopsy, MMT of biopsied muscle	24 y. o/thigh /5	18 y. o/rectus femoris/4	29 y. o/triceps/4
Atrophy of muscle	Upper limbs	Upper limbs	Upper limbs
Rimmed vacuole	None	None	Present
Immunohistochemistry	p62: negative	p62: diffuse fine granular deposits	p62: diffuse fine granular deposits
	TDP-43: negative	TDP-43: negative	TDP-43: diffuse fine and coarse granular deposits
	MHC-I: n.a.	MHC-I: sarcolemma	MHC-I: sarcolemma > sarcoplasm
	MHC-II: n.a.	MHC-II: n.a.	MHC-II: sarcolemma > sarcoplasm
Inflammatory cell infiltration	Mild	Mild	Moderate, CD4 or CD8-positive

Methods

Histochemical analyses

Muscle specimens from Cases 1 and 3 were fixed in 10% buffered formalin and paraffin-embedded blocks were prepared. Sections of 6 μm thickness were cut, deparaffinized and stained with haematoxylin and eosin (H&E) stain.

Frozen samples from Cases 2 and 3 were prepared. Sections of 10 μm thickness were cut in a rapid freezing manner and stored at -80°C until used. They were stained with H&E, modified Gömöri trichrome (mGT), cytochrome c oxidase (COX) and succinate dehydrogenase (SDH) stains.

Immunohistochemical analyses

The 6 μm -thick sections cut from paraffin-embedded blocks were deparaffinized and antigen was retrieved by autoclaving (20 min at 120°C) and using a heparinizing Histofine Antigen Retrieval Solution pH 6 (415281, Nichirei, Tokyo, Japan). The 10 μm -thick sections cut from the frozen samples were fixed in 100% acetone.

Treated sections were blocked with phosphate-buffered saline (PBS) containing 3% bovine serum albumin (BSA). They were incubated overnight with primary antibodies in PBS containing 3% BSA at 4°C . The antibody reaction was visualized with the peroxidase-polymer-based method using a Histofine Simple Stain MAX-PO kit (Nichirei, Tokyo, Japan) with a DAB Substrate Kit (SK 4100, Vector Laboratories).

The primary antibodies used in this study were the following: TDP-43 (rabbit polyclonal [Cat No. 10782-2-AP], Protein Tech, Tokyo, Japan; 1:2000), p62 (mouse monoclonal [Cat No. 610832], BD Biosciences, New Jersey, United States; 1:500), ubiquitin (rabbit polyclonal [Cat No. U5379], Sigma-Aldrich, St. Louis, Missouri, United States; 1:100), CD4 (goat polyclonal [Cat No. SC-1140], Santa Cruz Biotechnology, Texas, United States; 1:200), CD8 (mouse monoclonal [M7103], DAKO, Agilent, California, United States; 1:200), major histocompatibility complex (MHC)-I (mouse monoclonal [Cat No. M0736], DAKO, Agilent, California, United States; 1:200), MHC II (anti-HLA-DR [B308], Affinity BioReagents, Golden, Colorado, United States; 1:500), desmin (mouse monoclonal [M0760], DAKO, Agilent,

California, United States; 1:100), myotilin (mouse monoclonal [NCL-MYOTILIN], Novocastra, Leica Biosystems, Illinois, United States; 1:20), alpha-B-crystallin (mouse [Ab13496], Abcam, Cambridge, United Kingdom, 1:2500), LC3 (microtubule-associated protein light chain 3, rabbit polyclonal [PM036], MBL, Aichi, Japan, 1:1000), CD68 (mouse monoclonal [M0814], DAKO, Agilent, California, United States; 1:200), C5b-9 (membrane attack complex [MAC], mouse monoclonal [M0777], DAKO, Agilent, California, United States; 1:100), CD31 (rabbit polyclonal [11265-1-AP], proteintech, Illinois, USA; 1:1200), and proteasome 20S LMP7 (rabbit polyclonal [ab3329], Abcam, Cambridge, United Kingdom; 1:200).

For immunofluorescence staining, primary antibodies were detected with Alexa Fluor 488-labeled goat anti-mouse IgG (Molecular Probes, Eugene, Oregon, USA; 1:200). Slides were mounted with Vectashield (Vector Laboratories) and observed with a FLUOVIEW FV-1000 confocal laser scanning microscope (Olympus).

Ethical approval

Procedures involving the use of human material were performed in accordance with ethical guidelines set by the Kyoto University Graduate School of Medicine. All the material used in this study was obtained for diagnostic purpose and permitted for scientific use with written informed consent.

Results

Case 1

H&E staining showed mild mononuclear cell infiltration in the endomysium surrounding non-necrotic fibres and in the perivascular area surrounding the perimysium, as reported previously (Figure 1a) [11]. Immunostaining showed a small number of perivascular CD4-positive cells. No CD8-positive cells were observed. Neither abnormal sarcoplasmic aggregates nor vacuoles were observed by means of histochemistry or immunohistochemistry (Figure 2a).

Case 2

H&E staining showed necrotic fibres with phagocytosis (Figure 1b). mGT staining did not reveal any rimmed

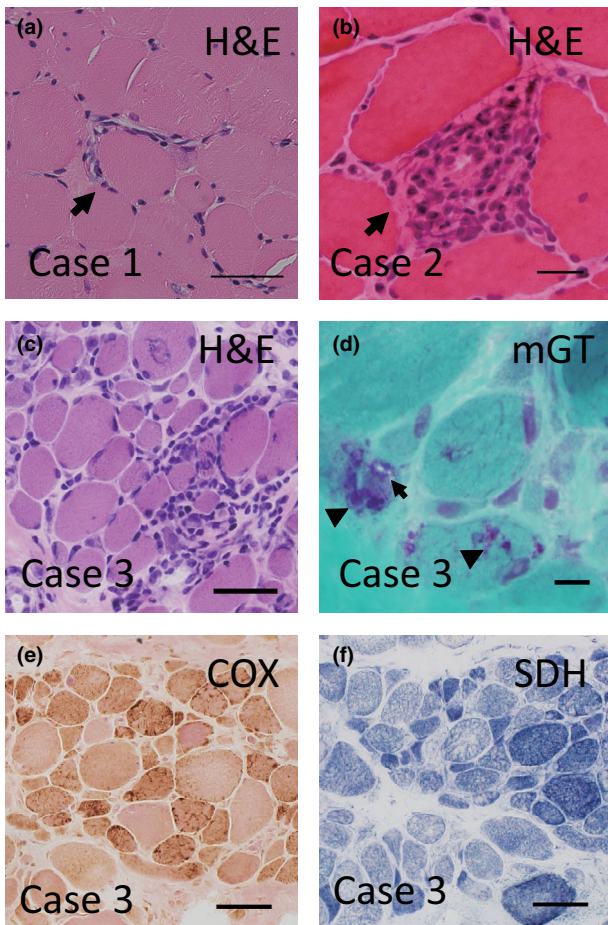


Figure 1. (a) Case 1: Infiltration of mononuclear cells surrounding a muscle fibre. H&E stain of paraffin section. (b) Case 2: Phagocytic mononuclear cells in a necrotic muscle fibre. H&E stain of frozen section. (c) Case 3: Moderate infiltration of mononuclear cells in the endomysium. H&E stain of frozen section. (d) Case 3: Rimmed vacuoles in muscle fibre (arrow) and cytoplasmic body (arrowhead). mGT stain of frozen section. (e) Case 3: COX expression was normal. (f) Case 3: SDH expression was normal. Abbreviations: H&E, haematoxylin and eosin; mGT, modified Gömöri trichrome; Scale bars: a, c 50 μ m; b 25 μ m; d 10 μ m; e, f, 50 μ m. [Colour figure can be viewed at wileyonlinelibrary.com]

vacuoles. p62-positive fine granular deposits were observed in a few myofibres by means of immunohistochemistry (Figure 2b). TDP-43 was present in the myonuclei without any abnormal deposits in the cytoplasm. Most muscle fibres expressed MHC-I in the sarcolemma (Figure 2c).

Case 3

H&E staining showed scattered necrotic and regenerating fibres. Endomyosial and perivascular mononuclear

cell infiltration was remarkable (Figure 1c). mGT staining revealed some fibres with cytoplasmic bodies and rimmed vacuoles in the cytoplasm (Figure 1d). COX (Figure 1e) and SDH (Figure 1f) expression were normal. Characteristically, myofibres with p62-positive and TDP43-positive diffuse fine granular deposits were scattered in the sarcoplasm. The staining of a few myofibres was more marked on the sarcolemma than on the sarcoplasm (Figure 2d,g). Most muscle fibres expressed MHC-I on the sarcolemma (Figure 2h); some fibres also expressed MHC-II more markedly on the sarcolemma (Figure 2i). Intracytoplasmic vacuoles were immunostained with anti-ubiquitin antibodies (Figure 2j). Infiltrating mononuclear cells were composed of CD4-positive (Figure 2k) and CD8-positive T cells (Figure 2l), and CD68-positive macrophages (Figure 2m). Myofibres with sarcolemmal MAC deposition were scattered (Figure 2n). Capillary dropout was not observed in the endomysium with immunohistochemistry for CD31 (data not shown). Muscle tissue from the three patients with NNS and from patients with other types of myositis (Table S1) were immunostained with a 20S Proteasome Subunit beta 5i antibody, but no apparent difference in staining was observed between these groups (Figure 2o,p).

The sarcoplasm did not express the myxovirus resistance protein A (MxA), a known diagnostic marker of dermatomyositis (data not shown) [13–15]

Discussion

Here, we assessed the clinical and myopathological features of three patients with NNS. The present three cases initially presented with a pernio-like rash and periodic high fever followed by myositis. All cases showed calcification of basal ganglia on a brain CT scan and some auto-immune antibodies. The three patients were treated with corticosteroids without any clinical effect. The common pathological feature was mononuclear cell infiltration in the endomysium and in the perivascular area, consisting of CD4- and CD8- positive T-cell infiltration and over-expression of MHC-I on myofibres. These findings confirmed that NNS could cause myositis (i.e. genetic inflammatory myopathy).

In cultured fibroblasts from NNS patients, mutant β 5i impairs immunoproteasome function and leads to accumulation of ubiquitinated proteins and oxidative

stress, which activate the phosphorylated p38 pathway and the secretion of IL-6 and IP-10, thereby leading to an inflammatory response [1]. This finding is further supported by a study that used myeloid cell lines derived from patient-derived induced pluripotent stem (iPS) cells [4]. In addition, serum levels of these

cytokines are elevated in patients with NNS, as well as in patients with CANDLE syndrome [1,16] Intriguingly, plasma IP-10 level is elevated in over 90% of patients with major idiopathic inflammatory myopathies, suggesting a common immunoserological feature between this type of myopathies and NNS/PRAAS [5].

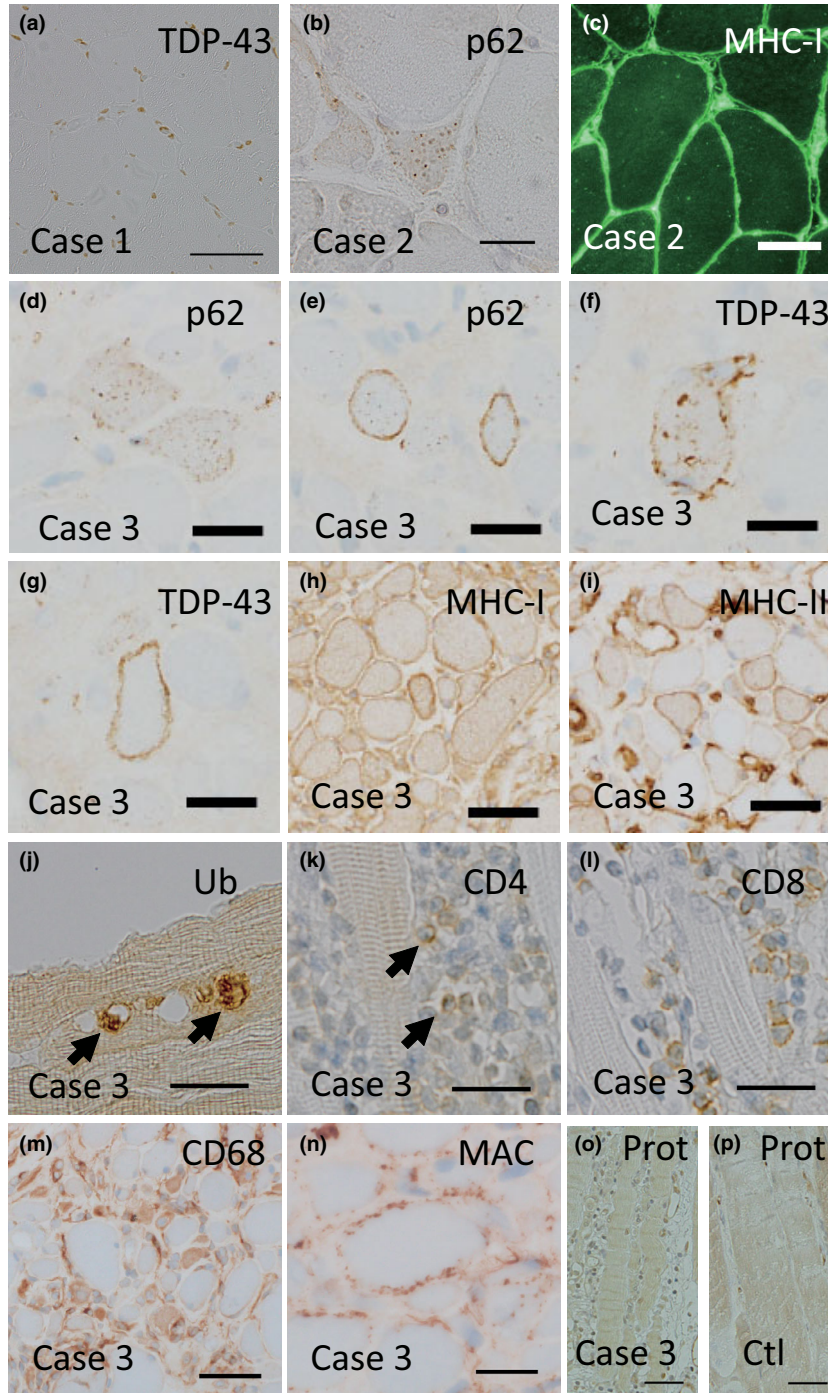


Figure 2. (a) Case 1: No aberrant sarcoplasmic TDP-43-positive aggregates are observed. Myonuclear staining can be seen physiologically in a paraffin section. (b) Case 2: p62-positive diffuse fine granular deposit in a muscle fibre of a frozen section. (c) Case 2: A frozen section showing MHC-I positive sarcolemma in almost all myofibres. (d) Case 3: A frozen section showing p62-positive diffuse fine granular deposit in muscle fibres. (e) Case 3: A frozen section showing more marked p62 stainability in the sarcolemma than the sarcoplasm of a few myofibres. (f) Case 3: A frozen section showing TDP-43-positive coarse granular deposit in a myofibre. (g) Case 3: Sarcolemma highlighted by TDP-43 in a frozen section. (h) Case 3: MHC-I positive sarcolemma and relatively mildly positive sarcoplasm in almost all myofibres shown in a frozen section. (i) Case 3: MHC-II positive fibres abundantly seen in a frozen section. (j) Case 3: Ubiquitin (Ub) positive vacuoles (arrows) in a muscle fibre of a longitudinal paraffin section. (k) Case 3: CD4-positive inflammatory cell infiltration (arrow) around a non-necrotic myofibre in a longitudinal paraffin section. (l) Case 3: Infiltration of CD8-positive inflammatory cells around a non-necrotic myofibre in a longitudinal paraffin section. (m) Case 3: CD68-positive macrophages around muscle fibres. (n) Case 3: Sarcolemmal deposition of MAC. (o) Case 3 of NNS, (p) Control myositis case: the muscles of an NNS case were faintly immunostained with an anti-20S Proteasome Subunit beta 5i antibody (Prot). The control similarly showed a faint staining pattern (number 3 in the Table S1, immune-mediated necrotizing myopathy positive for anti-signal recognition particle antibodies). Scale bars: a, c, h, i, m, o, p 50 µm; b, d–g, j–l 25 µm, n 20 µm. [Colour figure can be viewed at wileyonlinelibrary.com]

Immunoproteasome subunits $\beta 1i$ and $\beta 5i$ have been reported to regulate the expression of MHC-I in idiopathic inflammatory myositis [17]. In NNS cases, impairment of immunoproteasome function due to subunit $\beta 5i$ mutation could lead to increased expression of MHC-I as a result of a compensatory mechanism.

Another pathological feature observed was abnormal protein aggregation in sarcoplasm in Case 3, which was not seen in Cases 1 or 2. Case 3 had more severe inflammatory changes, while Cases 1 and 2 showed only mild mononuclear cell infiltration. The patient in Case 3 (29 years of age) was older than in Cases 1 and 2 (24 and 18 years of age, respectively), suggesting that abnormal protein aggregates may develop in more advanced stages when inflammatory changes are severe. Oyanagi *et al.* previously reported that the autopsied sample of a 47-year-old patient showed many myofibres with rimmed vacuoles, severe myofibre atrophy, and fibrosis of endomysium and perimysium in a discrete and multifocal distribution [12]. Ultrastructural observation revealed myeloid bodies, an increased number of degenerated mitochondria (some of which contained para-crystalline inclusions), and cytoplasmic bodies [12]. This case was later genetically confirmed as NNS [1]. These findings collectively suggest that the pathological features of NNS include inflammation and degeneration with abnormal protein aggregation.

p62 is known as an autophagy adaptor that recognizes ubiquitinated degenerative proteins and damaged mitochondria [18,19]. Alteration of autophagy, highlighted via a diffuse sarcoplasmic staining pattern by p62, is one of the characteristic features of immune-mediated necrotizing myopathy, which can exhibit severe muscle deficit and often requires intensive

immunosuppressive therapy [20]. Abnormal TDP-43 aggregation in muscle fibre was another feature of Case 3. TDP-43 is known to aggregate in motor neurons in amyotrophic lateral sclerosis [12,13]. TDP-43 and p62 are reported to aggregate in affected muscles in myositis [14], especially frequently in inclusion body myositis (IBM) [15]. IBM is a refractory myositis characterized by inflammation and rimmed vacuoles and is the commonest form of myositis in patients over 50 years of age. Interestingly, Cases 2 and 3 shared some pathological features with these diseases: endomysial CD8-positive cell infiltration, overexpression of MHC 1 and 2 in myofibres, and abnormal sarcoplasmic aggregates. These pathological features, particularly the accumulation of abnormal proteins, could underlie the refractory response to conventional immunosuppressive therapy. Further understanding of the inflammatory and degenerative processes of NNS would also help understand the pathomechanism of these refractory idiopathic inflammatory myopathies. It is noted that our group has recently established a patient-derived iPSC model of NNS [4,16]. Knowledge of NNS myopathological features will contribute to validating how well the iPSC model recapitulates the disease.

This study has some limitations. Ultrastructural data are lacking in this study, which could contribute to the delineation of pathological features, especially degenerative processes. However, samples for electron microscopy were not available. Another limitation is that Case 1 lacked MHC-I and MHC-II immunohistochemistry and Case 2 lacked MHC-II immunohistochemistry because of a shortage of available muscle samples. Likewise, we could not assess cytoplasmic bodies immunohistochemically. Moreover the present cases partially lacked profiles of myositis-specific autoantibodies or

myositis-associated autoantibodies, including the anti-cN1A antibody.

Conclusion

The muscle pathology of patients with NNS characteristically showed both inflammatory and degenerative features. Further studies to elucidate the pathomechanism of NNS will lead to the establishment of a therapeutic strategy for NNS, which would also help to develop a more effective therapy for other refractory idiopathic inflammatory myopathies with degenerative features.

Acknowledgements

This work was supported by the “MEXT KAKENHI Grant Number JP16K18383”, “The Practical Research Project for Rare/Intractable Diseases from the Japan Agency for Medical Research and Development (AMED) [TA, KM, NK, FF]”, and a “Wakayama Medical University Special Grant-in-Aid for Research Projects [KM, NK, MM]”.

Author contributions

TA, KM and NK designed the research. KO, KS, SK, RN and TS acquired the tissue specimens from the donor material. AU, FL, and MM assisted with microscopy image analyses. IN, SU, MU, FF, HI and RT gave feedback on the results of this work. TA wrote the manuscript, which was edited by all authors.

References

- 1 Arima K, Kinoshita A, Mishima H, Kanazawa N, Kaneko T, Mizushima T, et al Proteasome assembly defect due to a proteasome subunit beta type 8 (PSMB8) mutation causes the autoinflammatory disorder, Nakajo-Nishimura syndrome. *Proc Natl Acad Sci* 2011; **08**: 14914–9
- 2 Kanazawa N. Nakajo-Nishimura syndrome: an autoinflammatory disorder showing pernio-like rashes and progressive partial lipodystrophy. *Allergol Int* 2012; **61**: 197–206
- 3 Ohmura K. Nakajo-Nishimura syndrome and related proteasome-associated autoinflammatory syndromes. *J Inflamm Res* 2019; **12**: 259–65
- 4 Honda-Ozaki F, Terashima M, Niwa A, Saiki N, Kawasaki Y, Ito H, et al Pluripotent stem cell model of Nakajo-Nishimura syndrome untangles proinflammatory pathways mediated by oxidative stress. *Stem Cell Rep* 2018; **10**: 1835–50
- 5 Uruha A, Noguchi S, Sato W, Nishimura H, Mitsuhashi S, Yamamura T, Nishino I. Plasma IP-10 level distinguishes inflammatory myopathy. *Neurology* 2015; **85**: 293–4
- 6 Torrelo A, Patel S, Colmenero I, Gurbindo D, Lendínez F, Hernández A et al Chronic atypical neutrophilic dermatosis with lipodystrophy and elevated temperature (CANDLE) syndrome. *J Am Acad Dermatol* 2010; **62**: 489–95
- 7 Garg A. Lipodystrophies: genetic and acquired body fat disorders. *J Clin Endocrinol Metab* 2011; **96**: 3313–25. <https://doi.org/10.1210/jc.2011-1159>
- 8 Garg A, Hernandez MD, Sousa AB, Subramanyam L, De Villarreal LM, Dos Santos HG, et al An autosomal recessive syndrome of joint contractures, muscular atrophy, microcytic anemia, and panniculitis-associated lipodystrophy. *J Clin Endocrinol Metab* 2010; **95**: 58–63
- 9 Sanchez GAM, Reinhardt A, Ramsey S, Wittkowski H, Hashkes PJ, Berkun Y et al JAK1/2 inhibition with baricitinib in the treatment of autoinflammatory interferonopathies. *J Clin Invest* 2018; **128**: 3041–52
- 10 Tanaka M, Miyatani N, Yamada S, Miyashita K, Toyoshima I, Sakuma K, et al Hereditary lipo-muscular atrophy with joint contracture, skin eruptions and hyper- γ -globulinemia: a new syndrome. *Intern Med* 1993; **32**: 42–5
- 11 Kasagi S, Kawano S, Nakazawa T, Sugino H, Koshiba M, Ichinose K, et al A case of periodic-fever-syndrome-like disorder with lipodystrophy, myositis, and autoimmune abnormalities. *Mod Rheumatol* 2008; **18**: 203–7
- 12 Oyanagi K, Sasaki K, Ohama E, Ikuta F, Kawakami A, Miyatani N, et al An autopsy case of a syndrome with muscular atrophy, decreased subcutaneous fat, skin eruption and hyper γ -globulinemia: peculiar vascular changes and muscle fiber degeneration. *Acta Neuropathol* 1987; **73**: 313–9
- 13 Uruha A, Nishikawa A, Tsuburaya RS, Hamanaka K, Kuwana M, Watanabe Y, et al Sarcoplasmic MxA expression: a valuable marker of dermatomyositis. *Neurology* 2017; **88**: 493–500
- 14 Uruha A, Allenbach Y, Charuel JL, Musset L, Aussy A, Boyer O, et al Diagnostic potential of sarcoplasmic myxovirus resistance protein A expression in subsets of dermatomyositis. *Neuropathol Appl Neurobiol* 2019; **45**: 513–22
- 15 Inoue M, Tanboon J, Okubo M, Theerawat K, Saito Y, Ogasawara M, et al Absence of sarcoplasmic myxovirus resistance protein A (MxA) expression in antisynthetase syndrome in a cohort of 194 cases. *Neuropathol Appl Neurobiol* 2019; **45**: 523–4
- 16 Liu Y, Ramot Y, Torrelo A, Paller AS, Si N, Babay S, et al Mutations in proteasome subunit β type 8 cause chronic atypical neutrophilic dermatosis with lipodystrophy and elevated temperature with evidence of genetic and phenotypic heterogeneity. *Arthritis Rheum* 2012; **64**: 895–907

- 17 Bhattarai S, Ghannam K, Krause S, Benveniste O, Marg A, de Bruin G, et al The immunoproteasomes are key to regulate myokines and MHC class I expression in idiopathic inflammatory myopathies. *J Autoimmun* 2016; **75**: 118–29
- 18 Kraft C, Peter M, Hofmann K. Selective autophagy: ubiquitin-mediated recognition and beyond. *Nat Cell Biol* 2010; **12**: 836–41
- 19 Matsumoto G, Shimogori T, Hattori N, Nukina N. TBK1 controls autophagosomal engulfment of polyubiquitinated mitochondria through p62/SQSTM1 phosphorylation. *Hum Mol Genet* 2015; **24**: 4429–42
- 20 Fischer N, Preuß C, Radke J, Pehl D, Allenbach Y, Schneider U, et al Sequestosome-1 (P62) expression reveals chaperone-assisted selective autophagy in immune mediated necrotizing myopathies. *Brain Pathol* 2020; **30**: 261–71. <https://doi.org/10.1111/bpa.12772>

Supporting information

Additional Supporting Information may be found in the online version of this article at the publisher's web-site:

Table S1. List of control cases for immunocytochemistry with a 20S Proteasome Subunit beta 5i antibody.

Received 30 October 2019

Accepted after revision 29 February 2020

Published online Article Accepted on 6 march 2020